Direct Determination of the Magnetic Ground State in the Square Lattice $S = 1/2$ Antiferromagnet Li_2VOSiO_4

A. Bombardi,[1] J. Rodriguez-Carvajal,[2] S. Di Matteo,[3,4] F. de Bergevin,[1] L. Paolasini,[1] P. Carretta,[5] P. Millet,[6] and R. Caciuffo[7]

[1]*European Synchrotron Radiation Facility, BP 220, 38043 Grenoble Cedex 9, France*
[2]*Laboratoire Léon Brillouin, CEA-SACLAY, 91191 Gif sur Yvette Cedex, France*
[3]*Laboratori Nazionali di Frascati-INFN, via E. Fermi 40, I-00044 Frascati (Roma), Italy*
[4]*Dipartimento di Fisica "E. Amaldi," Università di Roma III, via della Vasca Navale 84, I-00146 Roma, Italy*
[5]*Istituto Nazionale per la Fisica della Materia and Dipartimento di Fisica, Università di Pavia, Via Bassi 6, I-27100 Pavia, Italy*
[6]*Centre d'Elaboration des Matériaux et d'Etudes Structurales, CNRS, 31055 Toulouse Cedex, France.*
[7]*Istituto Nazionale per la Fisica della Materia and Dipartimento di Fisica ed Ingegneria dei Materiali, Università Politecnica delle Marche, Via Brecce Bianche, I-60131 Ancona, Italy*

(Received 15 December 2003; published 7 July 2004)

Powder neutron diffraction and resonant x-ray scattering measurements from a single crystal have been performed to study the low-temperature state of the 2D frustrated, quantum-Heisenberg system Li_2VOSiO_4. Both techniques indicate a collinear antiferromagnetic ground state, with propagation vector $k = (\frac{1}{2}\ \frac{1}{2}\ 0)$, and magnetic moments in the a-b plane. Contrary to previous reports, the ordered moment at 1.44 K, $m = 0.63(3)\mu_B$, is very close to the value expected for the square lattice Heisenberg model ($\simeq 0.6\mu_B$). The magnetic order is three dimensional, with antiferromagnetic a-b layers stacked ferromagnetically along the c axis. Neither x-ray nor neutron diffraction shows evidence for a structural distortion between 1.6 and 10 K.

DOI: 10.1103/PhysRevLett.93.027202 PACS numbers: 75.25.+z, 61.12.–q

The phase diagram of two-dimensional (2D) frustrated quantum systems described by the Heisenberg Hamiltonian on a square lattice has been the subject of a number of theoretical analyses [1–3]. Thanks to the synthesis of several new compounds, such as $VOMoO_4$ [4], $Pb_2VO(PO_4)_2$ [5], Li_2VOGeO_4 [6], and Li_2VOSiO_4 [6], theoretical predictions can now be explored experimentally. Such a recently disclosed opportunity renewed the interest toward the so-called J_1-J_2 model, where J_1 and J_2 are the nearest- and the next-nearest-neighbor antiferromagnetic exchange integrals. In this model, depending on the $|J_2/J_1|$ ratio, different situations can occur. For $0.35 \leq |J_2/J_1| \leq 0.65$ a spin liquid or dimer ground state is predicted. For $|J_2/J_1| \leq 0.35$ an antiferromagnetic order should develop, whereas for $|J_2/J_1| \geq 0.65$ the ordering by the disorder mechanism [1,7,8] is expected to stabilize a twofold degenerate collinear order, with spins aligned ferromagnetically along the a axis and antiferromagnetically along the b axis, or vice versa. Some theoretical studies [1,2] suggested the possibility that such a twofold residual degeneracy leads to a finite-temperature Ising-like phase transition, with the chosen ground state being collinear or anticollinear [1]. However, coupling to the lattice may induce, as in the Jahn-Teller effect, a lattice distortion and remove the twofold degeneracy [9].

We explore such a scenario by making neutron powder-diffraction and resonant x-ray diffraction experiments on Li_2VOSiO_4, a system that has been proposed as a prototype of frustrated 2D quantum ($S = 1/2$) Heisenberg antiferromagnets, and one of the most studied among the new J_1-J_2 systems [9–13]. Like its Ge based counterpart, Li_2VOSiO_4 crystallizes in the tetragonal $P4/nmm$ space group, with 2 f.u. per cell and room temperature lattice parameters $a = 6.3682(6)$ Å and $c = 4.449(1)$ Å [6]. The magnetically active network of spin half V^{4+} ions is built up by layers of VO_5 square pyramids sharing corners with SiO_4 tetrahedra. The two V^{4+} ions occupy the positions $(\frac{1}{4}\ \frac{1}{4}\ z)$ and $(\frac{3}{4}\ \frac{3}{4}\ 1-z)$ with $z = 0.5861$. This structure suggests significant superexchange coupling both along the sides (J_1) and the diagonals (J_2) of the V^{4+} square lattice. Despite the small c value, the interlayer coupling should on the contrary be considerably weaker, so that Li_2VOSiO_4 should be a good example of a 2D system belonging to the intermediate $|J_2/J_1|$ region.

NMR, magnetization, specific heat, and muon spin rotation measurements on Li_2VOSiO_4 [10,11] indicate that a collinear antiferromagnetic structure is established below 2.8 K, with magnetic moments lying in the a-b plane, $J_2 + J_1 \simeq 8.2(1)$, and $J_2/J_1 \simeq 1.1(1)$. The analysis of these experiments leads to a strongly reduced value for the ordered magnetic moment, $m(T \rightarrow 0) \simeq 0.24\mu_B$, which is considerably smaller than that expected [14] for a nonfrustrated $S = 1/2$ system on a 2D lattice ($0.65\mu_B$). Just above T_N, ^{29}Si NMR results suggest the occurrence of a frustration-driven lattice distortion, which would relieve the degeneracy of the collinear ground state.

More recently some doubts were raised [12,13] concerning the actual value of the ratio J_2/J_1, which was found $\simeq 12$ from local density calculations. This result indicates that the system has a large J_2, rather than being

close to the border between the collinear and the dimer state. Moreover, it also immediately leads to a discrepancy with the reported value of $\simeq 0.24\mu_B$/V, too low for a large J_2 state. One possible reason for the reduction of the magnetic moment measured by ^{7}Li NMR is the fact that the calculation of its value was performed assuming an antiferromagnetic (AF) coupling in the c direction, whereas the actual coupling, as shown in the present Letter, is ferromagnetic (FM).

The actual value of the ordered magnetic moment is of central importance. A low value of m would clearly point to a sizable enhancement of the quantum fluctuations, as expected in the proximity of a quantum phase transition from the collinear to the spin-liquid (or dimer) state. On the other hand, a higher value of m would not exclude the possibility of having $J_2/J_1 \simeq 1.1(1)$, as theory shows an almost first-order change in the magnetic moment as a function of $|J_2/J_1|$, with m practically saturated at $|J_2/J_1| \geq 1$ [14].

The present study, combining neutron powder diffraction with resonant x-ray scattering (RXS) measurements on a single crystal, has allowed us to establish the low-temperature magnetic structure, which consists of collinear a-b AF layers stacked ferromagnetically along the c axis, and to directly measure the ordered magnetic moment, which is larger than previously reported [10,11], and consistent with $|J_2/J_1| \geq 1$, in good agreement with theoretical predictions [12,13].

The neutron powder-diffraction experiments were carried out on the high-resolution neutron diffractometer G4.2 [15] and the medium-resolution, high-intensity diffractometer G4.1 [16] of the Laboratoire Léon Brillouin in Saclay, France. The first instrument was operated with incident neutrons of wavelength $\lambda = 2.343$ Å and used to probe the occurrence of structural transformations. On the second diffractometer, neutrons with wavelength $\lambda = 2.426$ Å were used to determine the magnetic structure and the temperature dependence of the ordered moment. On both instruments, data were collected at several temperatures on warming from 1.44 to 30 K with the sample contained in a 8 mm cylindrical vanadium can inside a helium cryostat.

Rietveld [17] analysis of the diffraction patterns, show in Fig. 1, was performed using the crystallographic programs within the FULLPROF suite [18]. Refinements of high-resolution data confirm the structural model given in [6] for the paramagnetic phase. According to our experiments, there is no detectable structural phase transition when the sample is cooled below the Néel temperature T_N.

The magnetic structure has been solved by a systematic search, using the program BASIREPS [19] and the symmetry-representation analysis introduced by Bertaut [20] and developed by Izyumov and co-workers [21]. The angular positions of the observed magnetic Bragg peaks indicate that the magnetic unit cell has a propagation vector $\vec{k} = (\frac{1}{2}\ \frac{1}{2}\ 0)$. The corresponding basis states describing the magnetic moment on the vanadium sites were then identified, and the diffraction profiles, calculated for the various symmetry-allowed structures, were compared to the experimental one. The best fit has been obtained for states that transform as linear combinations of the basis vectors of the Γ_4 irreducible representation. However, powder diffraction does not allow us to distinguish between a collinear ([Fig. 2(a)] and a noncollinear [Fig. 2(b)] solution that gives equivalent diffraction profiles. In the collinear structure, the magnetic moments are oriented along [110] or along [1$\bar{1}$0]. These two choices correspond to having either paraller or antiparallel Fourier components of the magnetic moment carried by the two V ions $\vec{S}_{\vec{k}}(1) = m(\cos\phi, \pm\sin\phi, 0)$ and $\vec{S}_{\vec{k}}(2) = m(\pm\sin\phi, \cos\phi, 0)$, with $\vec{S}_{\vec{k}}(1)$ belonging to the V ion in $(\frac{1}{4}\ \frac{1}{4}\ z)$ and $\vec{S}_{\vec{k}}(2)$ belonging to that in $(\frac{3}{4}\ \frac{3}{4}\ 1-z)$. Here, ϕ is the angle between the magnetic moment $\vec{S}_{\vec{k}}(1)$ and the a direction in the crystal. The best fit to the powder-diffraction data is obtained assuming an ordered magnetic moment $m = 0.63(3)\mu_B$, both for the collinear and the noncollinear model. The intensity of the magnetic peaks in the diffraction pattern is proportional to the square of the magnetic moment. A value of $0.24\mu_B$ would give intensities smaller than the observed ones by a factor of about 5, well outside the experimental incertitude. Observed and calculated diffraction patterns are shown in Fig. 1. The final value of the magnetic Bragg R factor was $R = 17\%$. This relatively high value is due to the weakness of the magnetic reflections.

The ambiguity on the magnetic structure described above is lifted by the results of the RXS measurements performed with the ID20 beam line at the European Synchrotron Radiation Facility (ESRF), Grenoble, France [22]. The experiment was performed in the horizontal geometry, which implies incident photons with polarization parallel to the scattering plane (π). A

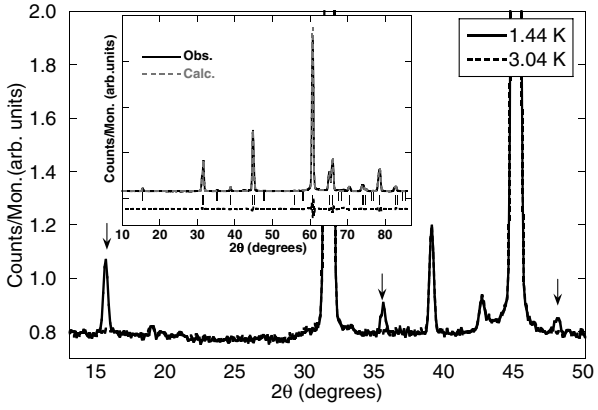

FIG. 1. Low-angle region of the powder diffraction patterns collected below and above T_N, at 1.44 and 3.04 K; the arrows mark the positions of the magnetic reflections. Observed and calculated diffraction patterns at 1.44 K are shown in the inset; the vertical lines are the positions of the peaks calculated by Rietveld refinement. The lower trace is the difference profile.

Li_2VOSiO_4 single crystal of about $3 \times 2 \times 0.1$ mm^3 was oriented with the larger face perpendicular to the $\langle 001 \rangle$ axis and the direction $\langle 110 \rangle$ in the scattering plane. A standard liquid-helium cryostat allowed the system to reach a base temperature of 1.44 K.

The first part of the experiment was dedicated to the search of structural distortions with a better resolution ($\Delta d/d = 0.005$) than that allowed by powder neutron diffraction. Using 9 keV photons together with a Ge analyzer we have monitored the position and width of the (105) and (113) charge reflections as a function of temperature. It must be noticed that we also performed an experiment on the BM16 high-resolution powder-diffraction beam line at the ESRF at 40 keV. The difference between the refined lattice parameters measured at 2 and 10 K was less than 5×10^{-5} Å $\simeq 1.3\sigma$, where σ is the experimental resolution and no changes were observed in the peak shapes. Thus we can conclude that, within the experimental errors, there are no structural variations on passing through T_N.

The second part of the experiment was performed around the V absorption K edge (5.465 keV), to measure the temperature dependence of the magnetic signal. A pyrolitic graphite (004) reflection was used to analyze whether the polarization of the scattered beam was parallel (π) or perpendicular (σ) to the scattering plane. Beam heating on the sample was a source of major difficulties with this experiment, due to the small value of the Néel temperature. To maintain the sample below T_N it was necessary to reduce the thermal load by inserting a 54 μm thick Al foil in the incident beam. With 5.465 keV photons, this reduces the incident flux to 13% of its maximum value. This flux still gave an appreciable heat load on the sample, but it was the best compromise to observe the very weak magnetic signal.

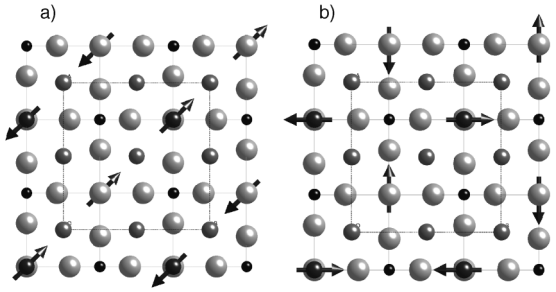

FIG. 2. Magnetic structures of Li_2VOSiO_4 projected along [001], as determined by neutron diffraction. The small black circles are the Si^{4+} ions, whereas the larger dark circles are the V^{4+} ions. Because of the VO_5 pyramid reversal, only one V over two is shown. The light grey circles are the O^{2-} ions and the dark grey circles are the Li^+ ions. The arrows show the configuration of the V^{4+} magnetic moments. (a) Collinear magnetic structure corresponding to $\vec{S}_{\vec{k}}(1) = m(\cos\phi, \sin\phi, 0)$ and $\vec{S}_{\vec{k}}(2) = m(\sin\phi, \cos\phi, 0)$ with $\phi = 45$. (b) Noncollinear magnetic structure, corresponding to $\vec{S}_{\vec{k}}(1) = m(\cos\phi, \sin\phi, 0)$ and $\vec{S}_{\vec{k}}(2) = m(\sin\phi, \cos\phi, 0)$ with $\phi = 0$.

RXS allows us to distinguish between the collinear and the noncollinear structures compatible with neutron powder-diffraction results. Indeed, the two V ions in the unit cell have different z coordinates, with $\Delta z \approx -0.1722 \sim -1/6$. Because of this difference, the magnetic contribution (both resonant and nonresonant) has a marked dependence on the angle ϕ that defines the magnetic structure. For instance, in the case of the $(\pm\frac{1}{2}\ \pm\frac{1}{2}\ 3)$ reflection, the projection of the magnetic moment perpendicular to the scattering plane is not accessible. As a result, the π-σ magnetic scattering is strong, whereas the π-π signal is very weak, whatever the value of ϕ. On the other hand, for the $(\pm\frac{1}{2}\ \pm\frac{1}{2}\ 2)$ reflection, a negligible π-π magnetic scattering is expected only for one of $\phi = 45°$ or $\phi = 225°$, i.e., for one of two equivalent collinear structures. As the experiment shows significant π-σ magnetic scattering for both $(\pm\frac{1}{2} \pm\frac{1}{2} 3)$ and $(\pm\frac{1}{2} \pm\frac{1}{2} 2)$ reflections, with no detectable π-π intensity, we can conclude that the structure is collinear, the sample being a magnetic monodomain, with either $\phi = 45°$ or $\phi = 225°$.

The integrated intensity of the magnetic $(\bar{\frac{1}{2}}\ \bar{\frac{1}{2}}\ 3)$ Bragg peak in the rotated polarization channel π-σ is shown in Fig. 3 as a function of the photon energy. Data were collected both below (closed squares) and above (open squares) the magnetic transition temperature. The fluorescence yield measured at 1.7 K is also shown, as an energy reference. At each energy, the intensity recorded below T_N is higher than that observed in the paramagnetic phase, due to the presence of a nonresonant magnetic contribution. In the pre-edge region, at $E = 5.467$ keV, a very narrow resonance is observed below

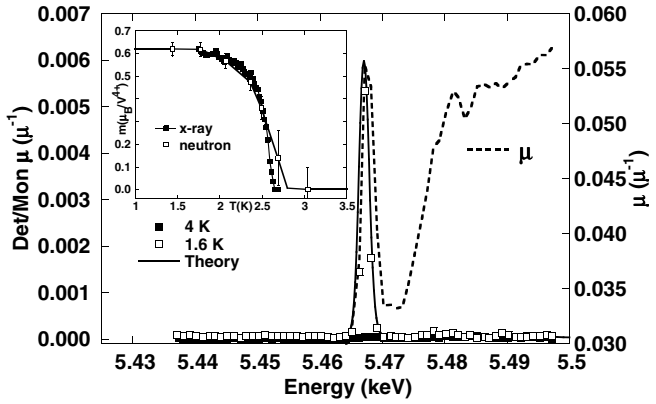

FIG. 3. Photon-energy dependence around the V K-absorption edge of the intensity of the $(\bar{\frac{1}{2}}\ \bar{\frac{1}{2}}\ 3)$ superlattice magnetic reflection. Data were collected in the rotated channel π-σ, above (open squares) and below (closed squares) the Néel temperature. Corrections for self-absorption have been applied. The fluorescence yield is shown by the broken line. The inset shows the temperature dependence of the ordered magnetic moment, m, as determined by neutron diffraction compared with the square root of the x-ray integrated intensity, after normalization at 1.44 K. The difference in the T_N has to be ascribed to the heat load on the sample.

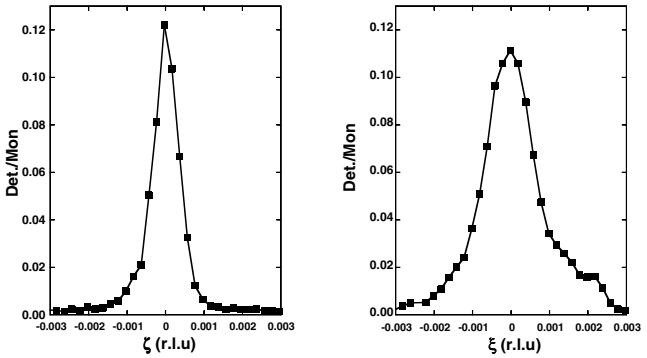

FIG. 4. Intensity of the $(\bar{\frac{1}{2}}\ \bar{\frac{1}{2}}\ 3)$ magnetic Bragg peak at the V K edge; π-σ polarization channel at $T = 1.6$ K. Left panel: $(\bar{\frac{1}{2}}\ \bar{\frac{1}{2}}\ 3 + \zeta)$ L scan; right panel $(\bar{\frac{1}{2}} + \xi\ \bar{\frac{1}{2}} + \xi\ 3)$ HH scan.

T_N, exactly at the same energy where the absorption coefficient (proportional to the fluorescence yields) exhibits a narrow peak. Similar peaks in the fluorescence spectra are well known [23] in V based compounds; they occur when the O_h symmetry around the V sites is reduced and the inversion center removed. In the absence of an inversion center, $3d$-$4p$ mixing is allowed and the electric-quadrupolar transition ($E2$, $1s \rightarrow 3d$) becomes dipole enhanced.

The absence of magnetic resonant scattering at higher energies (5480–5495 keV) is intriguing as it could be related either to a different magnetic symmetry or to a depleted magnetic density of states. We calculated the expected energy dependence by means of a relativistic extension of the FDMNES program [24,25] in the framework of multiple scattering theory and plotted it in Fig. 3 (solid line).

This result is consistent with the idea that only the filled part of the d band contributes to the magnetic moment [13], whereas the remaining magnetic density of state is depleted. The absence of any measurable resonant enhancement at the $4p$ energies can appear surprising when compared with the situation occurring in other V based compounds as V_2O_3 [26] and, to our best knowledge, in all the other reported $3d$ based compounds [27]. Such a difference could be either related to the different coordination, corundum in V_2O_3 and pyramidal in Li_2VOSiO_4, or to the different valences of V in the two compounds.

The RXS experiment allows us to probe directly the dimensionality of the magnetic structure. The width of a magnetic Bragg peak in a so-called L scan (intensity as a function of the wave vector offset along the $\vec{c}$ direction from the Bragg position) gives information on the correlation length along the c axis, while the in-plane correlation length is encoded in the width of the magnetic Bragg peak in an HH scan (intensity as a function of the wave vector offset along the $\vec{a} + \vec{b}$ direction). Figure 4 reports the results of such scans around the $(\bar{\frac{1}{2}}\ \bar{\frac{1}{2}}\ 3)$ magnetic Bragg peak. The intensity was measured at the V K edge in the π-σ channel, with the sample at 1.6 K. Both the L- and the HH scans give resolution limited peaks, with full width at half maximum comparable to those obtained in corresponding scans for structural Bragg peaks. This is proof that the magnetic ordering is long range both in the a-b plane and along the c direction with the lower limits to the correlation lengths being $\simeq 5500$ Å in the a-b plane and $\simeq 8500$ Å in the c direction. The magnetic structure is three dimensional, with the a-b magnetic layers aligned ferromagnetically in the c direction. An AF coupling along c is not compatible with the observed propagation vector, as there is no change of the unit cell in the c direction.

In conclusion, our measurements confirm the magnetic structure proposed in [10,11] but give a higher value for the ordered magnetic moment. This result suggests that Li_2VOSiO_4 is well inside the collinear state.

[1] C. L. Henley, Phys. Rev. Lett. **62**, 2056 (1989).
[2] P. Chandra *et al.*, Phys. Rev. Lett. **64**, 88 (1990).
[3] L. Capriotti *et al.*, Int. J. Mod. Phys. B **14**, 3386 (2000).
[4] P. Carretta *et al.*, Phys. Rev. B **66**, 094420 (2002).
[5] E. E. Kaul *et al.*, in Proceedings of The International Conference of Magnetism, Rome, 2003 [J. Magn. Magn. Mater. (to be published)].
[6] P. Millet and C. Satto, Mater. Res. Bull. **33**, 1339 (1998).
[7] E. F. Shender, Sov. Phys. JETP **56**, 178 (1982).
[8] J. Villain *et al.*, J. Phys. (Paris) **41**, 1263 (1980).
[9] F. Becca and F. Mila, Phys. Rev. Lett. **89**, 037204 (2002).
[10] R. Melzi *et al.*, Phys. Rev. Lett. **85**, 1318 (2000).
[11] R. Melzi *et al.*, Phys. Rev. B **64**, 024409 (2001).
[12] H. Rosner *et al.*, Phys. Rev. Lett. **88**, 186405 (2002).
[13] H. Rosner *et al.*, Phys. Rev. B **67**, 014416 (2003).
[14] H. J. Schulz *et al.*, J. Phys. I (France) **6**, 675 (1996).
[15] A. I. Kurbakov *et al.*, Mater. Sci. Forum **308**, 321 (2000).
[16] G. André, G4.1; for details, see http://www-llb.cea.fr/spectros/pdf/g41-llb.pdf.
[17] H. M. Rietveld, J. Appl. Crystallogr. **2**, 65 (1969).
[18] J. Rodríguez-Carvajal, Physica (Amsterdam) **55B**, 65 (1993).
[19] J. Rodríguez-Carvajal, BASIREPS; the program can be freely downloaded at ftp://ftp.cea.fr/pub/llb/divers/BasIreps.
[20] E. F. Bertaut, Acta Crystallogr. Sect. A **24**, 217 (1968).
[21] Yu. A. Yziumov, *Neutron Diffraction of Magnetic Materials* (Consultants Bureau, New York, 1991), p. 217.
[22] For details about the beamline ID20, see http://www.esrf.fr/exp_facilities/ID20/html/id20.html.
[23] J. Wong *et al.*, Phys. Rev. B **30**, 5596 (1984).
[24] Y. Joly, Phys. Rev. B **63**, 125120 (2001).
[25] Y. Joly, FDMNES; the program can be freely downloaded at http://www-cristallo.grenoble.cnrs.fr/simulation.
[26] L. Paolasini *et al.*, Phys. Rev. Lett. **82**, 4719 (1999).
[27] M. Takahashi *et al.*, Phys. Rev. B **67**, 064425 (2003).